Frontiers of Information Technology & Electronic Engineering
www.jzus.zju.edu.cn; engineering.cae.cn; www.springerlink.com
ISSN 2095-9184 (print); ISSN 2095-9230 (online)
E-mail: jzus@zju.edu.cn

Supplementary materials for

Yang YANG, Fanming HUANG, Dong YUE, 2025. Reinforcement learning based privacy-preserving consensus tracking control of nonstrict-feedback discrete-time multi-agent systems. *Front Inform Technol Electron Eng*, 26(3):456-471. https://doi.org/10.1631/FITEE.2300532

1 Example 2

Marine surface vessels are taken as another example. The topology is the same as that in Example 1, and the position control systems of marine surface vessels are (Fossen, 2002)

$$\begin{cases} \eta_i(k+1) = \eta_i(k) + \triangle T\big[R(\psi_i(k))\nu_i(k)\big], \\ \nu_i(k+1) = \nu_i(k) + \triangle T\big[-M^{-1}(C(\nu_i(k))\nu_i(k), \\ \qquad\qquad +D(\nu_i(k))\nu_i(k)) + M^{-1}\tau_i + M^{-1}\varpi_i\big], \\ y_i(k) = \eta_i(k), \end{cases} \tag{S1}$$

where $\eta_i = \big[\breve{x}_i, \breve{y}_i, \breve{\psi}_i\big]^{\mathrm{T}}$ represents the actual position in the Earth-fixed frame consisting of $(\breve{x}_i, \breve{y}_i)$ and yaw angle $\breve{\psi}_i \in \big[0, 2\pi\big]$, $\nu_i = \big[\breve{u}_i, \breve{v}_i, \breve{r}_i\big]^{\mathrm{T}}$ is the velocity vector in the body-fixed frame, and the variables $\breve{u}_i$, $\breve{v}_i$, and $\breve{r}_i$ represent, respectively, the forward velocity (surge), the transverse velocity (sway), and the angular velocity in yaw. Surge is decoupled from sway and yaw; $\tau_i = \big[\tau_{i,1}, \tau_{i,2}, \tau_{i,3}\big]^{\mathrm{T}}$ is the control input vector; $\varpi_i(k)$ is a vector representing disturbances due to wind, waves, and ocean currents in the body-fixed frame; $R(\breve{\psi}_i) = \begin{bmatrix} \cos\breve{\psi}_i & -\sin\breve{\psi}_i & 0 \\ \sin\breve{\psi}_i & \cos\breve{\psi}_i & 0 \\ 0 & 0 & 1 \end{bmatrix}$ is a rotation matrix; M is a non-singular, symmetric, and positive definite inertia matrix; $C(\nu_i)$ is the matrix of Coriolis and centripetal terms; $D(\nu_i)$ is the damping matrix.

In the simulation, $M = \begin{bmatrix} 25.8 & 0 & 0 \\ 0 & 24.6612 & 0 \\ 0 & 0 & 2.76 \end{bmatrix}$, $C(\nu_i) = \begin{bmatrix} 0 & 0 & 24.6612\breve{v}_i \\ 0 & 0 & 25.8\breve{u}_i \\ 24.6612\breve{v}_i & -25.8\breve{u}_i & 0 \end{bmatrix}$, and $D(\nu_i) = \begin{bmatrix} \breve{d}_{i,11} & 0 & 0 \\ 0 & \breve{d}_{i,22} & \breve{d}_{i,23} \\ 0 & \breve{d}_{i,32} & \breve{d}_{i,33} \end{bmatrix}$, where $\breve{d}_{i,11} = 0.7225 + 1.3274|\breve{u}_i| + 5.8664\breve{v}^2$, $\breve{d}_{i,22} = 0.8612 + 36.2823|\breve{v}_i| + 8.05|\breve{r}_i|$, $\breve{d}_{i,23} = -0.1079 + 0.845|\breve{v}_i| + 3.45|\breve{r}_i|$, $\breve{d}_{i,32} = -0.1052 - 5.0437|\breve{v}_i| - 0.13|\breve{r}_i|$, $\breve{d}_{i,33} = 1.9 - 0.08|\breve{v}_i| + 0.75|\breve{r}_i|$. $\varpi_i(k) = \big[1.3{+}2\sin(0.02k){+}1.5\sin(0.1k), -0.9{+}2\sin(0.02k - \pi/6){+}1.5\sin(0.3k), -\sin(0.09k + \pi/3) - 4\sin(0.01k)\big]$. The reference signal $\eta_d = \big[(4/7)\sin(t/7), (4/7)\cos(t/7), (1/7)\mathrm{atan}(4/7)\sin(t/7)\big]^{\mathrm{T}}$, and the initial states of the four followers are $\breve{x}_1(0) = -0.1$, $\breve{x}_2(0) = -0.2$, $\breve{x}_3(0) = -0.3$, $\breve{x}_4(0) = -0.35$, $\breve{y}_1(0) = 0.65$, $\breve{y}_2(0) = 0.7$, $\breve{y}_3(0) = 0.6$, $\breve{y}_4(0) = 0.9$, $\breve{\psi}_i = \pi/4$, $\breve{u}_i(0) = \breve{v}_i(0) = \breve{r}_i(0) = 0$. The parameter matrices are taken as $\breve{c}_{i,1} = \mathrm{diag}\big[5500, 5500, 5000\big]$ and $\breve{c}_{i,2} = \mathrm{diag}\big[600, 600, 500\big]$. $\triangle T = 0.05$.

The simulation results are shown in Figs. S1 and S2. The curves in the x, y, and ψ directions are plotted in Fig. S1. From Fig. S2, it is observed that the proposed strategy is able to force the ship to track the reference trajectory. In Fig. S3, we take the norm of the decryption errors in three directions, and it is evident that our method produces smaller decryption errors compared with the method in Liu (2013).

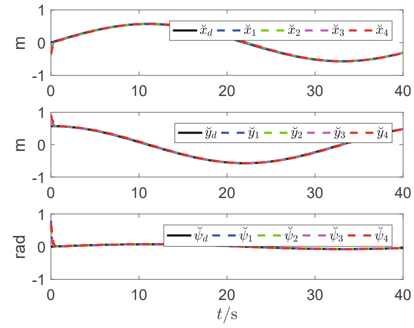

Fig. S1 Output consensus tracking performance of $\breve{x}_i$, $\breve{y}_i$, and $\breve{\psi}_i$ in Example 2

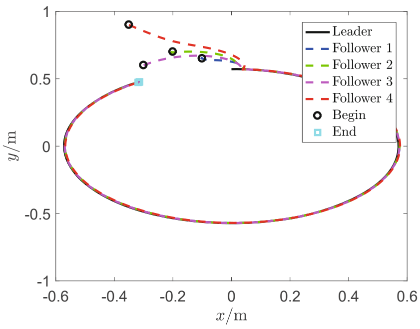

Fig. S2 Two-dimensional output consensus tracking in Example 2

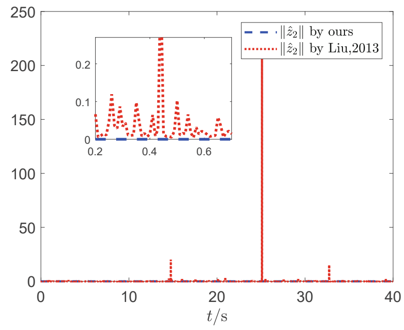

Fig. S3 Comparison of follower 2's decryption errors with different methods in Example 2

Reference

Fossen TI, 2002. Marine control systems-guidance, navigation, and control of ships, rigs and underwater vehicles. Marine Cybernetics, Trondheim, Norway.

Liu D, 2013. Homomorphic encryption for database querying. US2015295716A1. 2013-06-21.